



Experimental Analysis of Interface Temperature and Axial Shortening in Bi-Metallic Al-Cu Friction Welding

Kaunteya Ekatpure¹, M. V. Walame²
M-Tech student¹, Professor²

Vishwakarma institute of technology, Manmohan Park, Bibwewad Pune, India¹
Vishwakarma institute of technology, Chintamaninagar, Pune, India²

Abstract:

It is very difficult to weld the bi-metallic joints by conventional fusion welding due to disadvantages like large heat affected zone, weld cracks, porosity, wide difference in melting point, thermal mismatch. As friction welding is solid state process these defects are easily overcome. The experimental analysis of interface temperature, axial shortening, torque is carried out and results are compared with analytical values. The parameters used for experimentations are friction pressure, forging pressure and friction time. The experimental trials are conducted according to Taguchi L9 array. Regression analysis is used to investigate the relationship between response variables and predictor. The experimental results and analytical results are closely matching and hence analytical solutions can be effectively used for modelling friction welding process.

Keywords: Bi-metallic friction welding, interface temperature, axial shortening, Taguchi L9 array, regression analysis, experimental solution.

I. INTRODUCTION

Copper–aluminum joints are inevitable for certain applications due to unique performances such as higher electric conductivity, heat conductivity, corrosion resistance and mechanical properties [1]. Conventional fusions welding have disadvantages like large heat affected zone due to melting of base metal, weld cracks, porosity [2]. Joining of Bi-metallic metals by fusion welding is difficult because wide difference in melting point, thermal mismatch [2]. Friction welding is preferred as it is solid state joining process. There are few scientists who studied the process and developed the equations for temperature calculations. Cheng who utilized a finite difference method to calculate temperature distribution [3]. Rykalin gave the one dimensional heat flow model for infinite rod [4]. Midling and Grong's investigation is based on development of simple semi empirical heat flow model for the continuous drive friction welding, based on Rykanlin's infinite rod [5]. The analytical solution of material flow during the forge stage in friction welding have previously been investigated and reported by Rich and Roberts [6]. Francis and Craine conclusion is that the viscous fluid model provides the best representation of the material flow fields during continuous drive friction welding of steel tubes [5]. Midling and Grong gave the analytical equation for velocity flow and effective strain rate by using heat affected zone [5]. Comparatively less work is done in the area of bi-metallic weld interface temperature, torque and axial shortening. Hence in the present study we focused on interface temperature of weld specimen as it is required to maintain interface temperature below melting temperature of parent material whichever has least melting point. The torque is required to select the machine power.

II. EXPERIMENTAL ANALYSIS

Materials used for friction welding are C101 and 6063 Al. The rod diameter is 25 mm and length of rod is 70mm each. Before

welding the materials are cleaned with acids to remove oil and any other contaminations. After washing of materials the faces of the rods are machined exactly perpendicular to the axis of rod so that the perfect contact between rods can generate accurate heat. The copper rod is machined properly as it is not going to deform and will stay as it was before. The friction welding is carried out on a machine called FWT 12. The spindle motor is of 2000 rpm capacity. The forging cylinder is of capacity 200 bar with cylinder diameter 101.6 mm. All the machine parameters like rpm, friction pressure, forging pressure, friction time and forging time are computer controlled. The friction welding machine operates in two modes burn off mode and time mode. In burn off mode the loss in length is defined and in time mode time is defined. Following welding is done in time mode as the considered parameters are in time. The aluminium rod is held in chuck to the spindle side as shown in FIGURE 1(a). For different diameter machine has different collets. The copper rod is held in cup which is hydraulically operated. The cup assembly is mounted on rail and it can also travel in transverse direction. The forging force is applied by cylinder as shown in FIGURE 1(b).



a. Holding cup



b. Cylinder

FIGURE 1. HOLDING CUP AND CYLINDER ASSEMBLY

The total number of weld specimens carried are twelve. In this there are nine trials from Taguchi L9 array. The welded specimens with collar are shown in FIGURE 2 (B). According to Taguchi L9 array each trial has specific combination of parameters which gives different collar and dimensions of

welded specimens. The interface temperature is measured by using non-contact type thermometer. The actual welding occurs at contact region and more importantly the plastic deformation occurs at contact region. Hence it is very difficult to measure the temperature by using contact type thermal sensor. The interface temperature is measured with the non-contact type infrared thermometer as shown in FIGURE 2 (A).

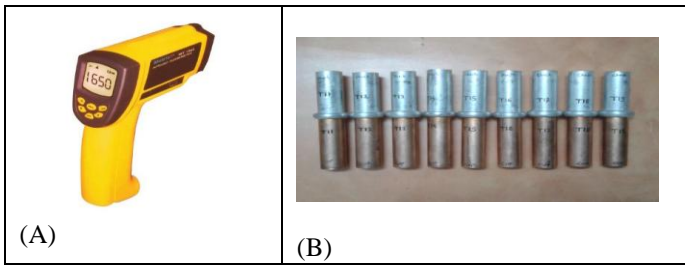


FIGURE.2. FRICTION WELDING (A). NON-CONTACT TYPE IR THERMOMETER, (B). WELDED SPECIMENS

III. DESIGN OF EXPERIMENT

In industry, designed experiments can be used to systematically investigate the process or product variables that influence product quality. After you identify the process conditions and product components that influence product quality, you can direct improvement efforts to enhance a product's manufacturability, reliability, quality, and field performance. Our area of interest will be on Taguchi L9 array for experimental trials and regression analysis.

3.1 TAGUCHI L9 ARRAY

A Taguchi design, or an orthogonal array, is a method of designing experiments that usually requires only a fraction of the full factorial combinations. An orthogonal array means the design is balanced so that factor levels are weighted equally. Because of this, each factor can be evaluated independently of all the other factors, so the effect of one factor does not influence the estimation of another factor. After selecting the Taguchi design select the number of factors and design level, as for our area of interest select 3 for both level and factor. The Minitab will show you available designs for selected level and factor combinations. The Taguchi L9 orthogonal array is created with the help of Minitab software. The TABLE 1 indicates the three level and three factor Taguchi design.

TABLE 1. TAGUCHI L9 ARRAY

Trial	Friction Pressure (bar)	Forging Pressure (bar)	Friction time (sec)
11	25	55	0.3
12	25	60	0.5
13	25	65	0.7
14	30	55	0.5
15	30	60	0.7
16	30	65	0.3
17	35	55	0.7
18	35	60	0.3
19	35	65	0.5

3.2 REGRESSION ANALYSIS

Regression analysis is used to investigate and model the relationship between a response variable and one or more predictors. The Minitab software is used to calculate regression model. Use to add interaction terms and polynomial terms to

your model. By default, the model contains only the predictor variables that you entered in the main dialog box. Click 'Default' to return to this model at any time. To add terms to the model, select at least one predictor or term. To select multiple items, press the 'Ctrl' key while you click the predictors and/or terms. The basis of this approach is the assumption of a simplified linear model for the optimisation parameter η given by equation (1).

$$\eta = b_0 + b_1x_1 + b_2x_2 + b_3x_3 \tag{1}$$

Where x_1, x_2, x_3 etc, are the factors on which η depends and b_0, b_1, b_2, b_3 etc, represent the 'true' values of the corresponding unknowns. From the results of an experiment comprising a finite number of trials, one can arrive at sample estimates of the coefficients, b , which are then usually fitted into a linear regression equation (1) of the type. In simple terms, each coefficient represents the influence of the corresponding factor on the quality of the weld expressed by the optimisation parameter.

IV. RESULT AND DISCUSSION

5.1 TEMPERATURE RESULTS

The final temperature profile is the combination of the two stages i.e. heating stage and cooling stage. The analytical solution for heating stage and cooling stage is given by Midling [5]. The equation (2) and equation (3) indicates the heating and cooling stage temperature.

$$T_{max} - T_0 = \frac{q_0 \sqrt{t_h}}{A \rho C \sqrt{\pi \alpha}} \tag{2}$$

$$T - T_0 = \frac{q_0 \sqrt{t_h/t_s}}{A \rho C \sqrt{\pi \alpha}} (\sqrt{t} - \sqrt{t - t_s}) \tag{3}$$

Where, q_0 is the net power, C is the volume heat capacity ($J/mm^3 \text{ } ^\circ C$), α is the thermal diffusivity (mm^2/s), t_h is the heating time, A is cross section area od rod, t_s is the welding time. The analytical representation of temperature profile along with experimental representation is given in FIGUTRE 3.

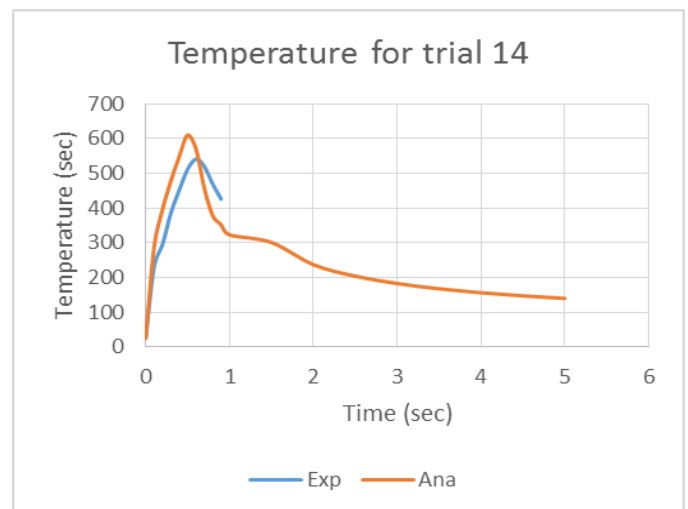


FIGURE .3. TEMPERATURE PROFILE FOR TRIAL 14

From FIGURE 3 we can see that analytical results show maximum temperature than experimental results. This is because of the assumptions made during solution. The analytical calculations are based on one dimension heat transfer and heat loss due to conduction and convection is neglected. The error calculations are given in TABLE 2.

TABLE 2. ERROR CALCULATION

Trial	T ana	T exp	Error (ana)
11	402.43	360	11.78611
12	512.26	403	27.11166
13	601.54	498	20.79116
14	609.72	541	12.7024
15	716.84	601	19.27454
16	477.12	417	14.41727
17	832.32	689	20.80116
18	553.15	495	11.74747
19	707.47	624	13.3766

From the graphs shown in FIGURE 4 and FIGURE 5 it can be concluded that maximum interface temperature increases with increase with friction time and friction pressure. The increase in temperature is because of the increase in rate of heat generation.

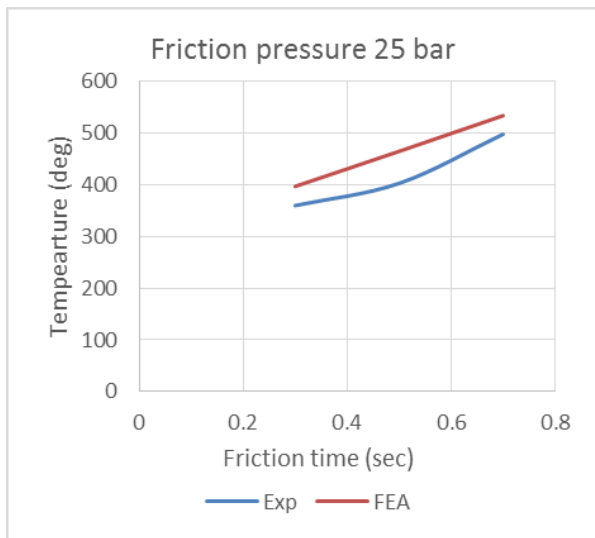


FIGURE.4.EFFECT OF FRICTION TIME ON TEMPERATURE

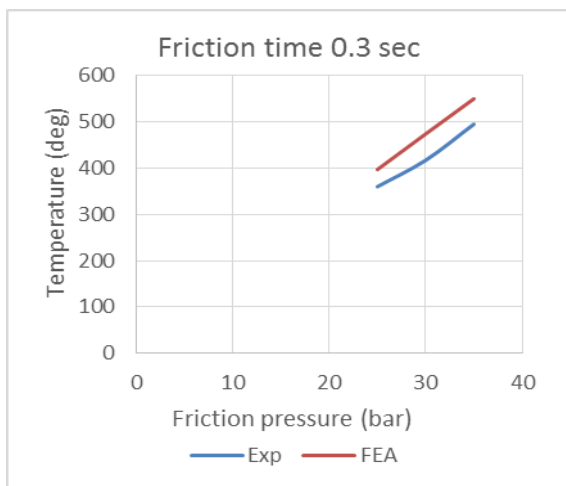


FIGURE.5. EFFECT OF FRICTION PRESSURE ON TEMPERATURE

Regression equation for the temperature is calculated by using Minitab. The R-sq value indicates that the predictors explain 98.60% of the variance in Interface temperature. The adjusted R-sq is 98.13%, which accounts for the number of predictors in the model. Both values indicate that the model fits the data well. Because the predicted R-sq value is close to the R-sq and adjusted R-sq values, the model does not appear to be overfit and has adequate predictive ability. The p-values for the

estimated coefficients of FP and t are both 0.000, indicating that they are significantly related to response. The p-value for FG is 0.5, indicating that it is not related to Temperature. Additionally, the sequential sum of squares indicates that the predictor FG doesn't explain a substantial amount of unique variance. This suggests that a model with only FP and t may be more appropriate. Normal probability plot of residuals shows the straight line indicating the residuals are normally distributed. Residuals versus fits this plot should show a random pattern of residuals on both sides of '0'. A positive correlation is indicated by a clustering of residuals with the same sign. A negative correlation is indicated by rapid changes in the signs of consecutive residuals.

Regression Equation

$$\text{Interface (T)} = -229.9 + 19.43 \text{ FP} + 345.0 \text{ t}$$

5.2 AXIAL SHORTENING

The axial strain rate is the main cause for axial shortening. The analytical solution for axial strain rate is given by Midling [5]. The analytical solution for axial shortening is given in equation (3). The experimental axial shortening compared with analytical solution in TABLE 3.

$$\epsilon_{zz} = \frac{-2\alpha v_0}{R} \left[1 - \left(\frac{z}{h} \right)^\rho \right] \tag{3}$$

Where where α is a dimensionless term, v_0 is the measured rate of axial displacement during friction welding (mm/s), R is the specimen radius (mm), Z is the axial distance (mm), h is the total width of the plasticized region (mm), ρ is a dimensionless parameter depending on the configuration of the up-set collar

TABLE. 3. COMPARISON OF AXIAL SHORTENING BY ANALYTICALLY AND EXPERIMENTALLY

Trial	e _{zz}	loss (ana)	Loss (exp)	Error (%)
11	0.18904	3.799	3	26.64
12	0.3192	6.287	4.7	33.77
13	0.34495	7.161	6.4	11.89
14	0.24262	4.927	3.7	33.17
15	0.46024	9.278	7.7	20.49
16	0.37934	5.765	5.2	10.87
17	0.29456	6.053	4.5	34.51
18	0.32959	6.614	5.5	20.70
19	0.35827	7.319	6.3	16.18

The heat generation will soften the more amount of Al. This will increase the collar dimensions. So the increased collar dimensions will also increase the axial strain rate. The FIGURE 12 shows the effect of friction time on axial shortening.

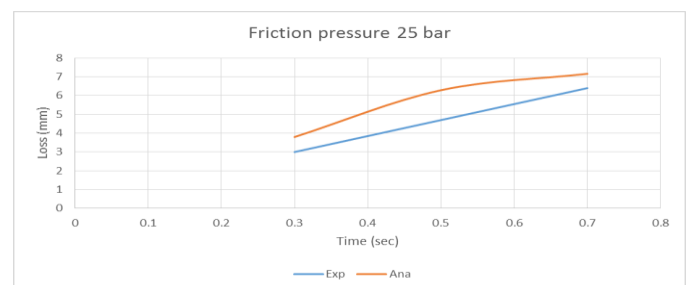


FIGURE.6. EFFECT OF FRICTION TIME ON AXIAL SHORTENING AT DIFFERENT FRICTION PRESSURE

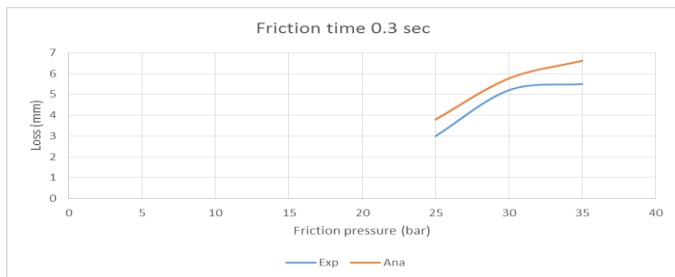


FIGURE 7. EFFECT OF FRICTION PRESSURE ON AXIAL SHORTENING

From figure 6 and 7 we can see that with increasing friction pressure and friction time the axial shortening also increases.

The p-value for the regression model in the Analysis of Variance table (0.000) shows that the model estimated by the regression procedure is significant. The p-values for the estimated coefficients of FP, FG, and t are zero, indicating that they are significantly related to response. The R-sq value indicates that the predictors explain 99.55% of the variance in Interface temperature. The adjusted R-sq is 99.28%, which accounts for the number of predictors in the model. Both values indicate that the model fits the data well. Because the predicted R-sq value is close to the R-sq and adjusted R-sq values, the model does not appear to be overfit and has adequate predictive ability. Normal probability plot of residuals shows the straight line indicating the residuals are normally distributed. Residuals versus fits this plot should show a random pattern of residuals on both sides of '0'. A positive correlation is indicated by a clustering of residuals with the same sign. A negative correlation is indicated by rapid changes in the signs of consecutive residuals.

Regression Equation

$$\text{Axial shortening} = -9.708 + 0.07333 \text{ FP} + 0.17333 \text{ FG} + 4.417 \text{ t}$$

5.4 TORQUE CALCULATION

The analytical solution for torque acting on rod given by Debroy [7].The analytical equation for torque acting on rod is given equation 4.

$$T = \frac{2\pi R^3}{3} [(1 - \delta)\tau + \delta\mu P_N] \tag{4}$$

Where δ is a dimensionless slip rate, P_N normal pressure, R radius of rod, μ coefficient of friction, τ shear stress at yielding. The temperature dependant shear strength (τ) of Al is given by Johnson-Cook material model. The constants of J-C equation for aluminium is given in TABLE 4 [13].

TABLE 4. JOHNSON-COOK MATERIAL MODEL CONSTANTS FOR AL 6063 [13].

A (MPa)	B (MPa)	n	C	m	T _{melt} (deg)
111.82	241.40	0.415	0.012	1.003	650

From TABLE 5 the error between calculated torque and experimental torque is because of constants assumed in Johnson-Cook model. Another reason for the error is difference in material properties. Analytical torque is more than experimental because at interface there is phenomenon called asperity melting. This molten layer reduces the coefficient of friction.

TABLE 5. ERROR CALCULATION FOR TORQUE

Trial	τ (Mpa)	Torque (Exp)	Torque (Ana)	Error (%)
11	18.413	67.2	75.286	12.03
12	15.409	54.5	63.001	15.59
13	12.080	46.3	49.391	6.67
14	10.374	53.6	42.415	20.86
15	9.956	48.1	40.435	15.37
16	14.55	54.9	59.514	8.40
17	9.549	46.9	39.865	16.75
18	12.549	46.9	51.308	9.39
19	9.349	49.8	38.500	23.24

The value of torque is greatly influenced by friction time and friction pressure because these two parameters directly affect the material properties. The effect of friction time and friction pressure given in FIGURE 8.

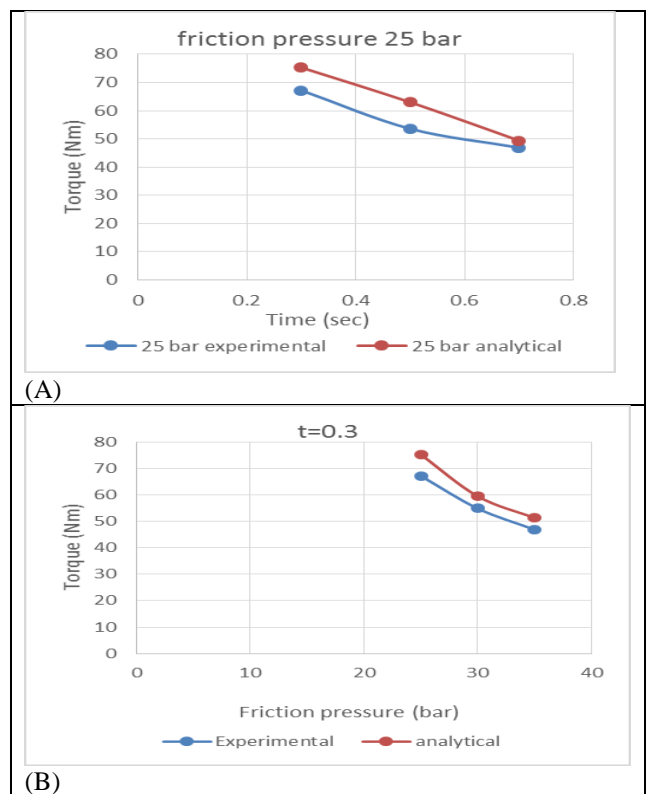


FIGURE 8. (A)EFFECT OF FRICTION TIME ON TORQUE, (B) EFFECT OF FRICTION PRESSURE ON TORQUE

The friction time and friction pressure is inversely proportional to torque as shown in FIGURE 8. This relation between torque and FP-time is because of softening of material according Johnson-Cook model. The p-value for the regression model in the Analysis of Variance table (0.000) shows that the model estimated by the regression procedure is significant. This indicates that at least one coefficient is different from zero. The p-values for the estimated coefficients of FP, t are both 0.000, indicating that they are significantly related to response. The p-value for FG is 0.35, indicating that it is not related to Temperature. Additionally, the sequential sum of squares indicates that the predictor FG doesn't explain a substantial amount of unique variance. This suggests that a model with only FP and t may be more appropriate.

The R-sq value indicates that the predictors explain 92.27% of the variance in Interface temperature. The adjusted R-sq is 92.36%, which accounts for the number of predictors in the model. Both values indicate that the model fits the data well. The predicted R-sq value is 93.70%. Because the predicted R-sq value is close to the R-sq and adjusted R-sq values, the model does not appear to be overfit and has adequate predictive ability.

Regression Equation

$$\text{Torque} = 94.3 - 0.338 \text{ FP} - 27.25 t$$

V. CONCLUSIONS

1. From the graphs shown in FIGURE 3 it can be concluded that maximum interface temperature increases with increase with friction time and friction pressure.

2. The P-value for interface temperature indicates that the interface temperature does not depend on forging pressure. From figure P-value for forging pressure is 0.5. Hence for the regression equation we neglect the forging pressure.

3. The P-value for torque indicates that the torque does not depend on forging pressure. From figure P-value for forging pressure is 0.32. Hence for the regression equation we neglect the forging pressure.

3. Analytical results for temperature shows higher temperature than experimental. This is because analytical solution does not account for heat loss. (Convection loss and conduction loss).

4. From FIGURE 2 (B) can be seen that the axial shortening on the aluminium side is more than that on copper side. Thus, the aluminium material has experienced weld flash at the interface. This is due to the fact that melting point of aluminium is lower than that of copper.

5. The friction time and friction pressure is inversely proportional to torque as shown in FIGURE 8. This relation between torque and FP-time is because of softening of material according Johnson-Cook model.

VI. REFERENCES

- [1] Mumin Sahin. Joining with friction welding of high-speed steel and medium-carbon steel. *Journal of Materials Processing Technology* 168 (2005) 202–210.
- [2] I. Bhamji, R. J. Moat, M. Preuss, P. L. Threadgil, A. C. Addison and M. J. Peel. Linear friction welding of aluminium to copper. *Institute of Materials, Minerals and Mining* (2012) vol 17.
- [3] Cheng, C. J. 1962. Transient temperature distribution during friction welding of two similar materials in tubular form. *Welding Journal* 41(12): 542-s to 550-s
- [4] N. N. Rykalin, A. I. Pugin, and V. A. Vasireva, *Weld. Prod.* 6, 42 (1959).
- [5] O. T. Midling, O. Grong. A process model for friction welding of Al-Mg-Si alloys and Al-SiC metal matrix composites I. haz temperature and strain rate distribution. *Acta metall, mater.* Vol. 42, No. 5, pp. 1595-1609, 1994.

[6]. T. Rich and R. Roberts, *Weld. J.*, pp. 137s-145s (1971).

[7] A. Arora, T. DebRoy, H.K.D.H. Bhadeshia, Back-of-the-envelope calculations in friction stir welding – Velocities, peak temperature, torque, and hardness, *Acta Materialia* 59 (2011) 2020–2028.

[8] Wenya Li, Achilles Vairis. Linear and rotary friction welding review. *International Materials Reviews* (2016) ISSN: 0950-6608, 1743-2804.

[9] Mumin. Joining of aluminium and copper materials with friction welding. *Int J Adv Manuf Technol* (2010) 49:527–534

[10] Bekir S. Yilba, Ahmet Z. Sahin, Nafiz Kahraman, Ahmed Z. Al-Garni. Friction welding of St-A1 and Al-Cu materials. *Journal of Materials Processing Technology* 49 (1995) 431-443.

[11] I. Bhamji, R. J. Moat, M. Preuss, P. L. Threadgil, A. C. Addison and M. J. Peel. Linear friction welding of aluminium to copper. *Institute of Materials, Minerals and Mining* (2012) vol 17.

[12] M. Maalekian, E. Kozeschnik, H.P. Brantner, H. Cerjak. Comparative analysis of heat generation in friction welding of steel bars. *Acta Materialia* 56 (2008) 2843–2855

[13]. L. Kruska, Ł. Anaszewicz, J. Janiszewski, and M. Grażka. Experimental and numerical analysis of Al6063 duralumin using Taylor impact test. *EPJ Web of Conferences* 26, 01062 (2012)

VII. ACKNOWLEDGMENT

To put an effort like this requires the determination and help of many people around me and I would not be doing justice to their efforts by not mentioning each helping hand in person. I would like to thank Mr. Vipul Kulkarni, Friction welding technology, Pune-411023, for extending all possible help for experimentation.